Vol. 9(32), Apr. 2019, PP. 4154-4169

Contents list available at IJMEC

International Journal of Mechatronics, Electrical and Computer Technology (IJMEC)

Journal Homepage: www.aeuso.org

PISSN: 2411-6173 - EISSN: 2305-0543

Study of a Standalone Microgrid with Multiple Distributed Energy Resources

Anjali Torgal[1], Harsha Anantwar[2], K. Shanmukha Sundar[2]

[1]*Student Dayananda Sagar College of Engineering*

[2]*Faculty Dayananda Sagar College of Engineering*

Phone Number: *+91- 9611916640*

****Corresponding Author's E-mail:*** *torgalanjali@gmail.com*

Abstract

A standalone hybrid microgrid with Photovoltaic(PV), Wind energy conversion system(WECS), Diesel generator and a battery backup unit is investigated in this paper. A simple Power Management Strategy(PMS) is implemented and the performance of the microgrid is studied under different climatic and load conditions. A control strategy is implemented to control active(P) and reactive power(Q) of the microgrid. The quality of power is studied for different types of load. The results show that the proposed strategy can maintain the power quality in the hybrid microgrid without the support of the utility grid and is capable of supplying uninterrupted power to the load even under changing conditions of load. The results also demonstrate coordination between the PV MPPT and power control loop. MATLAB/SIMULINK is used for simulation.

Keywords: *Active power and reactive power control, Boost converter, Distributed energy resources(DERs), Energy Storage System(ESS), Fuzzy Logic Controller, Inverter, Maximum power point tracking(MPPT), Power management strategy(PMS), State of charge(SoC)*

1. Introduction

A standalone microgrid is an independent electric supply system powered exclusively by Distributed Energy Resources(DERs) with a Energy Storage System(ESS) for backup. Unlike conventional microgrids which are connected to the utility, these standalone microgrids are capable of supplying the load demand without the support of the utility grid and are therefore not connected to them. A major issue pertaining synchronization and control arises when DERs are integrated with the grid[1][2][3]. This issue is eliminated when DERs function independent of the grid. However, such a system faces its own difficulties with respect to control and power quality. This paper shows strategies that can to solve these issues and provide uninterrupted, quality power to the load. The system under consideration consists of the following sources: PV panel, WECS, diesel generator and a lead-acid battery as back up for PV. This paper is split into two parts. The first part demonstrates the PMS and the second part deals with active and reactive power control. So far the work done by various scholars in this direction incorporates either of the two parts of research[4][5][6][7][8][9][10]. This paper brings together two of the most important concerns related with standalone microgrids and suggests solutions for the two. Most three phase supplies are used to power static as well as dynamic loads in an industrial or domestic environment. The behavior of the system is investigated for static load(RL load) and dynamic load(Induction motor) load.

Article History:
Received Date: Dec. 19, 2018
Accepted Date: Mar. 16, 2019
Available Online: Apr. 01, 2019

The structure and focus of this paper is on the MPPT for the PV using a fuzzy logic controller, PQ control for the PV, strategy to control SoC of the battery, pitch angle control of the WECS and overall PMS

1.1 PV Panel

The Photovoltaic panel consists of several PV cells arranged in series and parallel to meet the requirements of output voltage, current and ultimately power[22][23][24][25][26]. The PV cell can be represented mathematically using the one diode equivalent model as shown in Fig. 1.

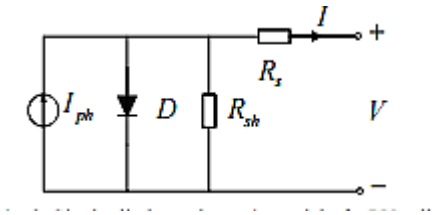

Fig. 1. Single diode model of PV cell

The relationship between current and voltage in the single-diode equivalent circuit is:

$$I=Iph-Is(e^{(((qV+IRs))/\Delta kT)-1)-(V+IRs)/Rsh} \quad (1)$$

where, Iph is photocurrent; Is is diode saturation current; q is coulomb constant (1.602e-19C); k is Boltzman's constant (1.381e-23 J/K); T is cell temperature (K); A is P-N junction ideality factor; Rs and Rsh are intrinsic series resistances. The PV panel considered in this system is the Kyocera GT200 panel with 125 strings in parallel and 4 cells in series per string. The total output power capacity of the panel is 100kW[2]. The characteristics of current and power are nonlinear with varying irradiance and temperature. Fig.2. shows the nature of current and power with change in irradiance at 25 deg centigrade temperature. The nature of current and power with change in temperature at 1000W/m2 irradiance is shown in Fig.3.

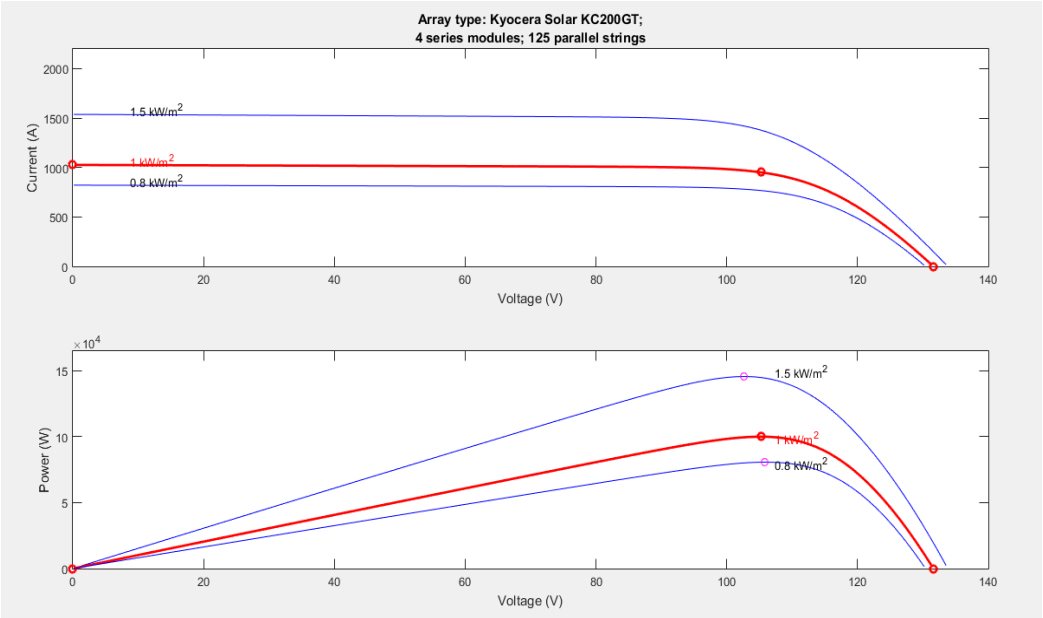

Fig. 2. I-V characteristics and P-V characteristics of Kyocera GT200 for varying irradiance at STC

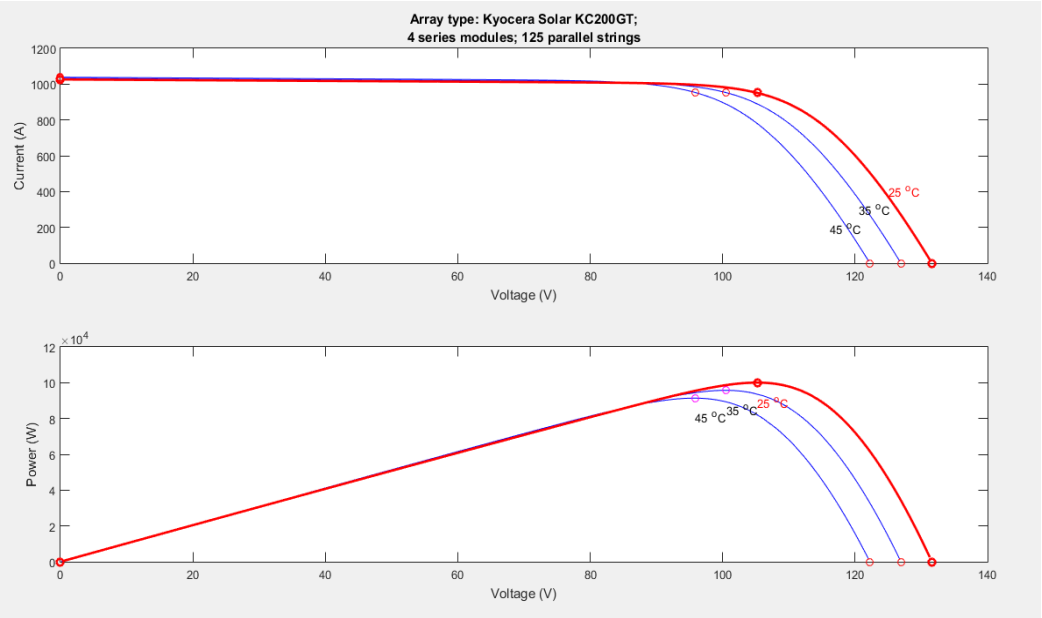

Fig. 3. I-V characteristics and P-V characteristics of Kyocera GT200 for varying temperatures at 1000W/m2 irradiance

The parameters of a single PV cell of Kyocera GT200 are shown in Table.1.

Table 1. Kyocera GT200 parameters at 1000W/m^2 irradiance and 25ºC

P_{MPP}	200.143W
V_{MPP}	26.3V
I_{MPP}	7.61A
V_{OC}	32.9V
I_{SC}	8.21A

1.2 DC-DC Boost converter

Fig.4. shows the circuit diagram of a dc-dc boost converter. The relationship between output voltage Vo and input voltage Vi is given by equation (2)

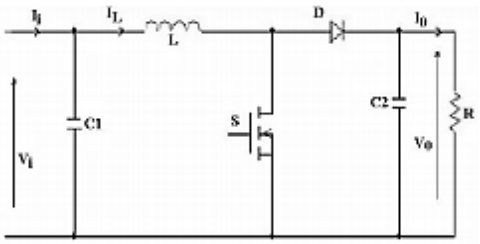

Fig. 4. Boost converter circuit

$$Vo/Vi=(1/(1-D)) \quad (2)$$

The output voltage can be controlled by varying the duty cycle D as observed from equation (2). The converter operates in two modes. First when switch is closed, the inductor gets charged by the source. The current trough inductor is assumed to be linearly varying for simplicity. The capacitor on load side discharges and supplies power to the load. The diode restricts back flow of current. The second mode

is when switch is open. The diode is forward biased. The inductor discharges and charges the capacitor along with the source and meets the load demands. The load current variation is very small and is considered in designing. For designing the inductor and capacitor the following equations are used:

For inductor

$$L=(Vo*D)/(\Delta I*f) \quad (3)$$

For capacitor

$$C_2=D/(R*(\Delta Vo/Vo)*f) \quad (4)$$

Where R is load resistance, f is the switching frequency, ΔVo/Vo is the output ripple voltage and ΔI is variation in load current. C_1 is chosen to achieve smooth DC at input of converter. The design parameters of the boost converter are as shown in Table.2.

Table 2. DC-DC boost converter parameters

L	2.323mH
C_2	1mF
F	20kHz

The switch is controlled by providing PWM pulses with the help of a FLC based MPPT controller for the PV panel. Input membership functions are change in current and change in power whereas change in duty cycle is the output membership function. The rule base applied to the FLC are as shown in the Table.3.

Table 3. Fuzzy rule base

Δd	ΔP				
ΔI	NH	NL	ZZ	PL	PH
NH	NH	NL	NL	ZZ	ZZ
NL	NL	ZZ	ZZ	ZZ	PL
ZZ	ZZ	ZZ	ZZ	PL	PH
PL	ZZ	PL	PL	PL	PL
PH	PL	PL	PH	PH	PH

1.3 Battery

A Lead-acid battery of 100kW capacity is chosen to provide backup to the PV panel for up to 1 hour at full load[20][21][22][23][24]. The battery is charged with the PV panel when load demand is low. SOC of 20% to 80% is maintained. If the Ppv is greater than Pbat, Ppv supplies to the load and vice verse. Fig. 5. Shows the selection criteria between PV and battery. The bidirectional converter used for battery is shown in Fig. 6.

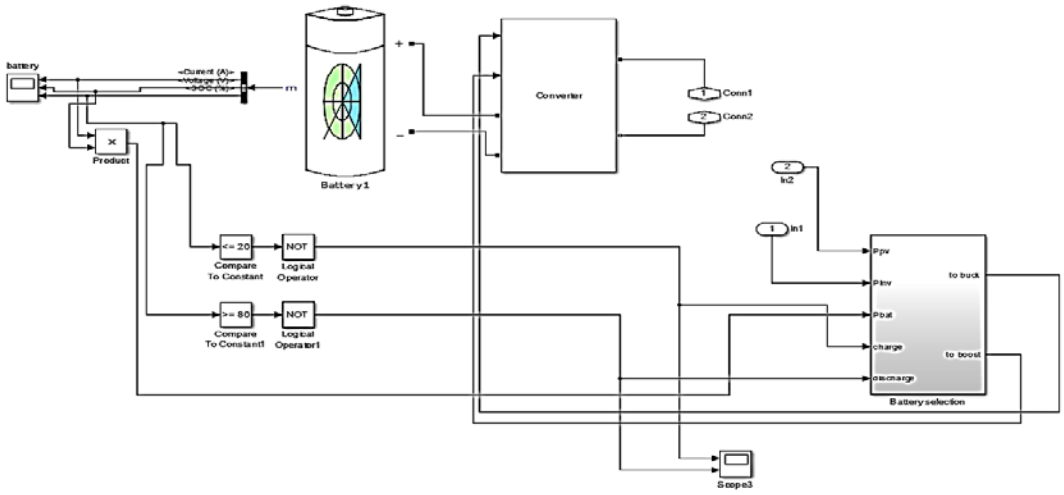

Fig. 5. Selection criteria between PV and battery

Switch 1 is ON in buck mode when the battery is charging while Switch 2 is OFF. Switch 2 is ON during boost mode when battery is discharging and Switch 1 is OFF.

1.4 WECS

A variable speed wind turbine with Permanent Magnet Synchronous Generator(PMSG) is used. The capacity of the WECS at wind speed of 12m/s is 100kW[27]. Fig. 7 shows the MATLAB model based design of the wind turbine. This model is used to generate the torque required for the PMSG. The readily available PMSG model in MATLAB is used. The output of the WECS is rectified and connected to the common inverter used to supply three phase AC to the load.

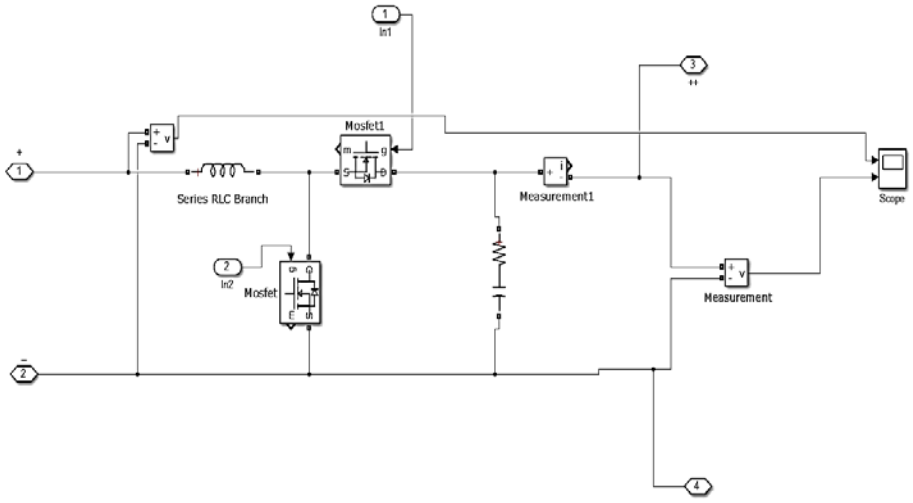

Fig. 6. Bidirectional converter for battery charging and discharging

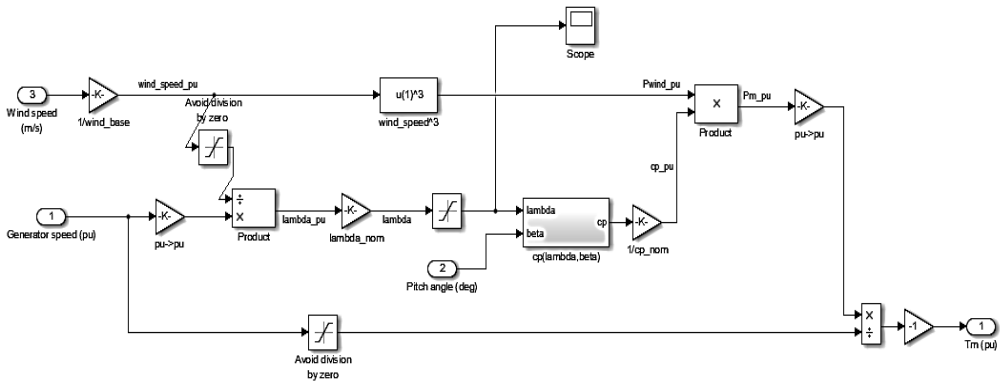

Fig. 7. MATLAB model based design of the wind turbine

1.5 Diesel generator

To facilitate full back up, a 100kW diesel generator set is provided to ensure uninterrupted power supply is a scenario when both PV and WECS are incapable to supply enough load and battery is completely discharged.

2. PROPOSED MODEL

The model under study is as shown in Fig. 8

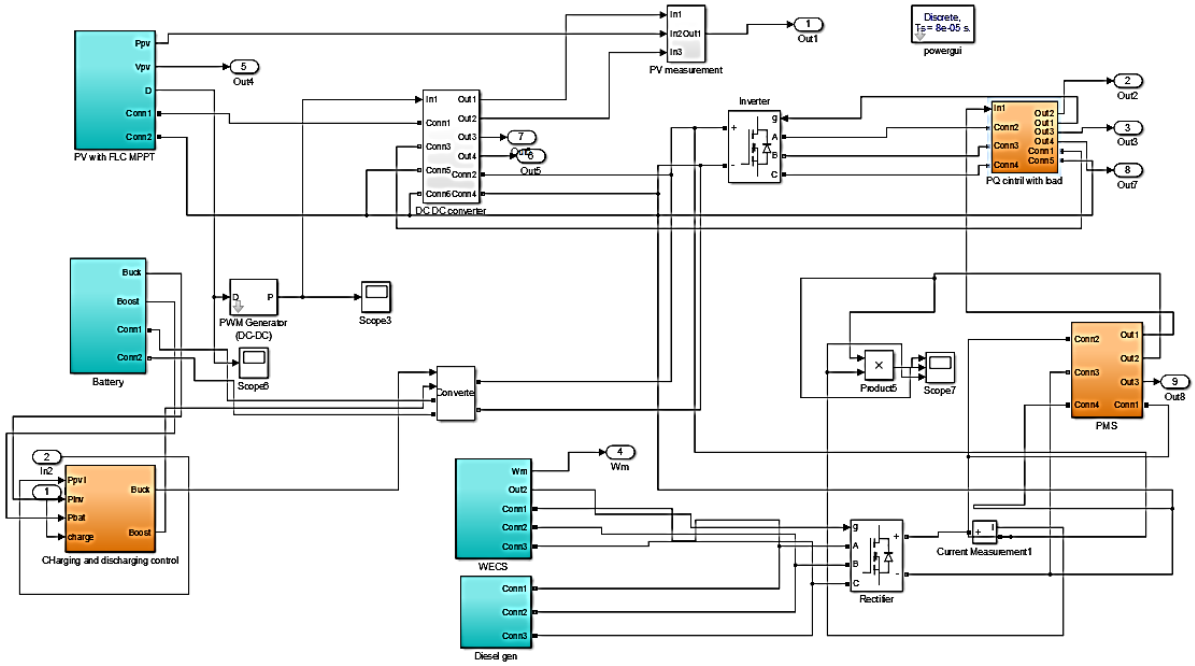

Fig. 8. MATLAB/SIMULINK model of the system under study

2.1 Power management strategy

When multiple resources are connected to a single point of common coupling, it is important to manage them in a way that the load demand is met. Block diagram of the model under study is as shown in Fig. 9

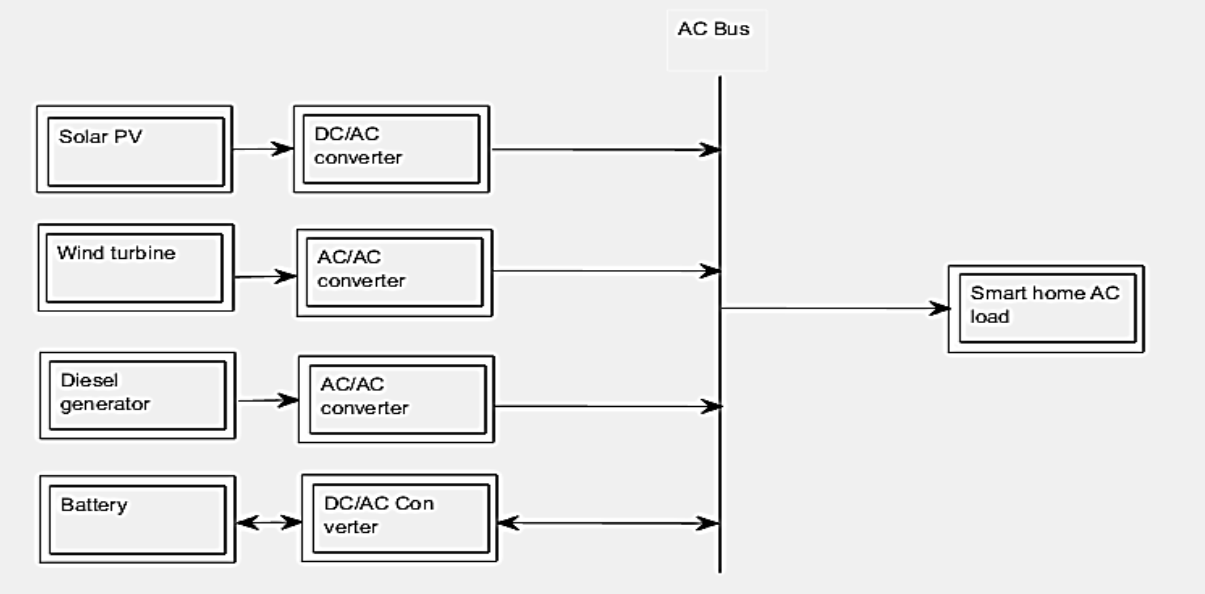

Fig. 9. Model diagram of grid-connected hybrid energy systems (HES) comprising a small micro grid with energy storage system

A priority is assigned to each of the resources to meet the load demand. The priority is as explained in the following algorithm:

- Measure the power generated by Solar, WECS, Battery, Diesel and the power demand of the load.
- If power generated by PV panel is equal to load demand, PV alone supplies to the load.
- If PV power is greater than the load, PV alone supplies to load and also charges the battery if Battery SOC is less than 80%.
- If PV power is less than demand, battery discharges and supplies to load until battery SOC reaches 20%.
- If power of PV is less than load demand, battery SOC is 20% or less and WECS power is greater or equal to load demand, WECS alone supplies to the load.
- If power PV, battery and WECS is less than load demand, Diesel generator alone supplies to the load.

2.2 Active and reactive power control

Particulary when the PV panel is supplying to the load which has the highest priority as a source in this model, the control of active and reactive power is necessary. Three PI controllers are used for this. It is carried out as shown in Fig. 10

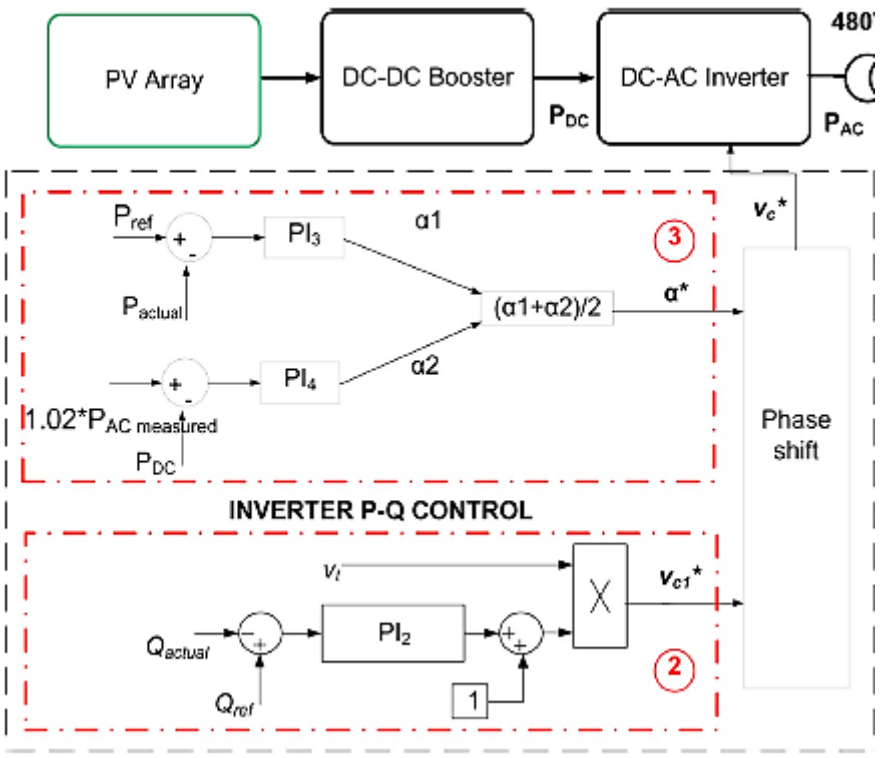

Fig. 10. PQ control strategy for PV [2]

3. RESULTS

The results after integrating the wind along with the PV and battery system while the system is in standalone mode are shown below. Fig. 11 shows the output of the inverter when it is fed by the PV panel alone. Two cases are demonstrated when battery is getting charged and discharged.

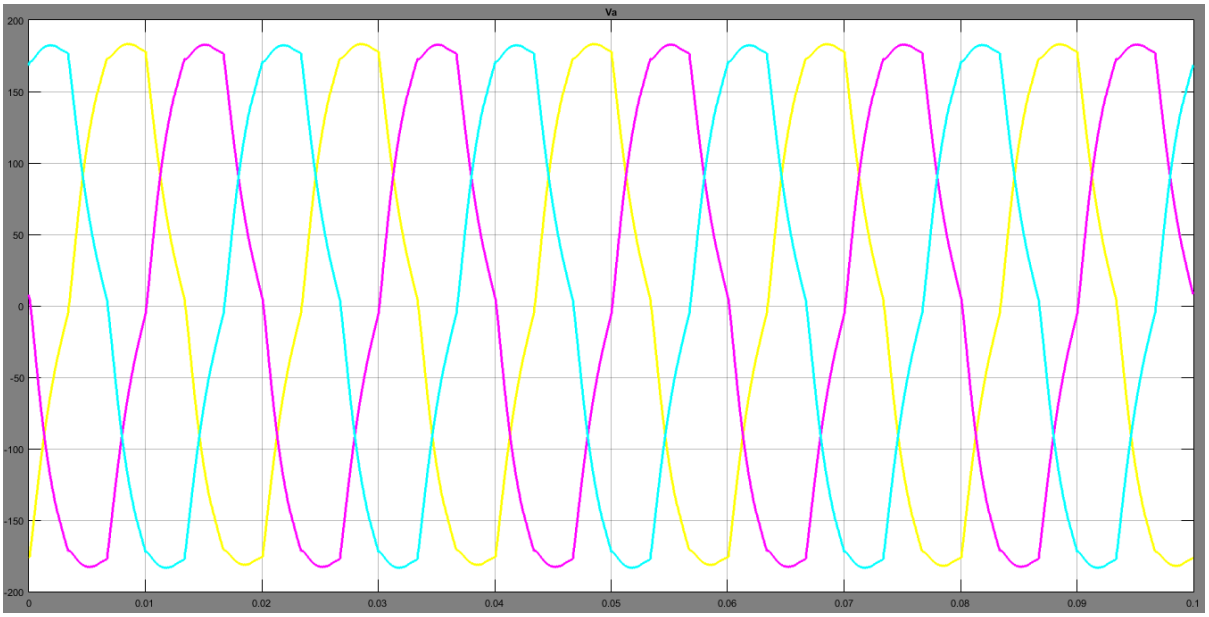

Fig. 11. Output of inverter when PV is feeding the load

The Fig. 11 shows the three phase voltage output of the inverter. The inverter is feeding the 1Kw load. LC filter with L=1mH and C= 100microF have been employed to achieve smooth sinusoidal output waves. Time in seconds is on X-axis and Voltage in volts is on Y-axis.

The output power of PV panel is as shown below in Fig. 12. The voltage settles to 2.72kW after 0.02 seconds. The irradiance is taken to be constant at 1000W/m2 and temperature is 25deg C.

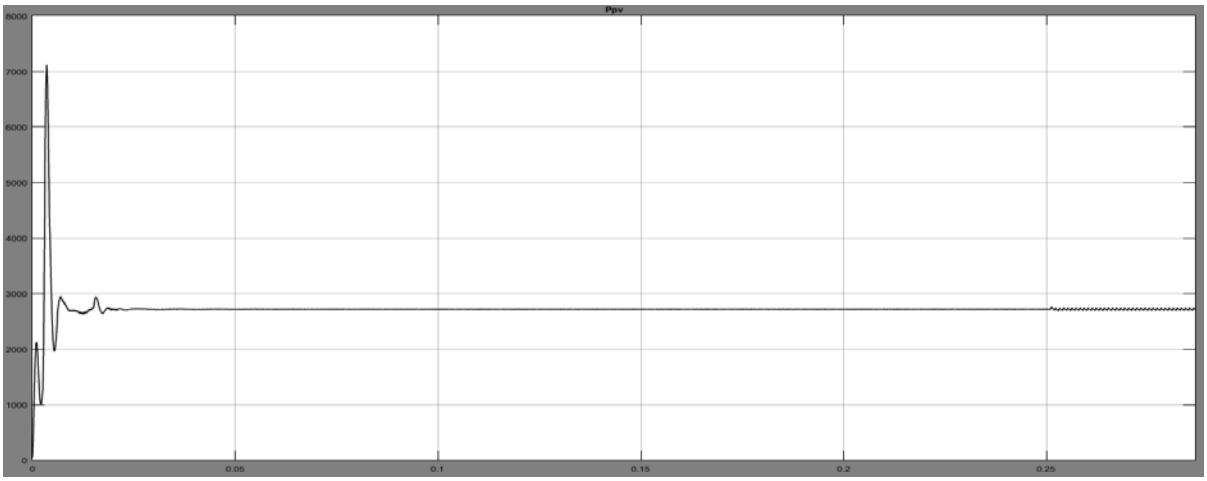

Fig. 12. Output of PV panel with irradiance 1000W/m2 and temperature 25deg C

The PV output in a scenario where it is sufficient to supply to the load and excess power charges the battery is shown above in Fig.12. Time in seconds is on X-axis and Power output from PV panel magnitude is on Y-axis. The settling time is observed to be around 0.023 seconds from the figure.

Fig.13 shows the selection of Buck mode for battery as the power generated by the PV panel is greater than that of battery power.

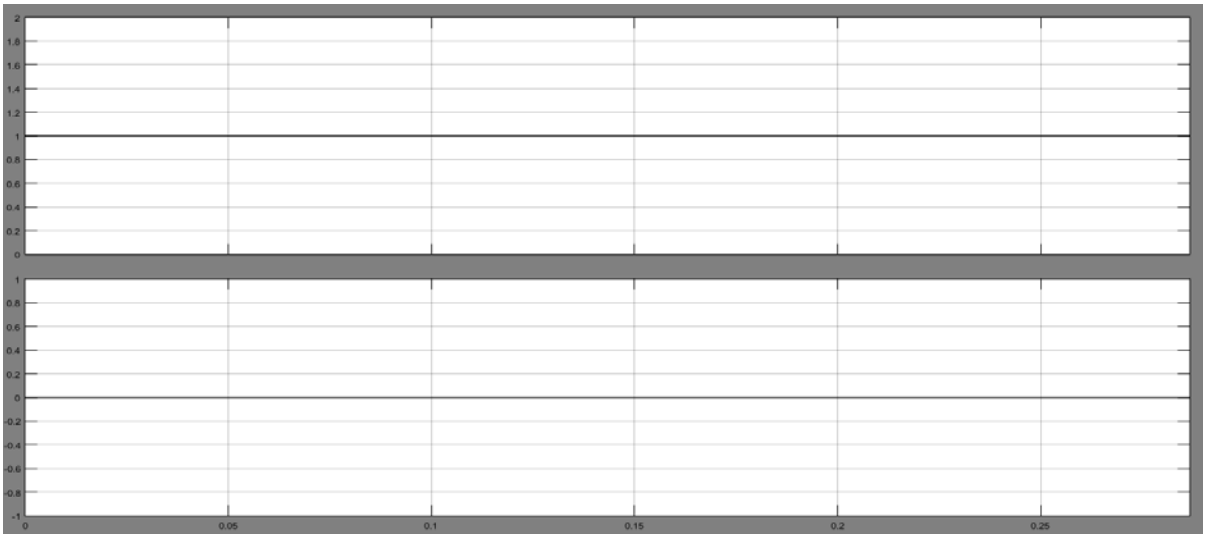

Fig. 13. Selection criteria for battery

Since the selection criteria between multiple sources is important, Fig. 13 is shown to demonstrate the duration in which the battery is in buck mode, that is it is getting charged with the excess power generated from PV panel. Time is on X-axis in seconds and on the Y-axis, the first waveform shows a high for the given duration which corresponds to gate pulses to the buck switch in the bidirectional converter connected to battery. We can observe that the Boost signal continues to remain in low state for this duration. Fig.14 shows the battery SOC, current and voltage.

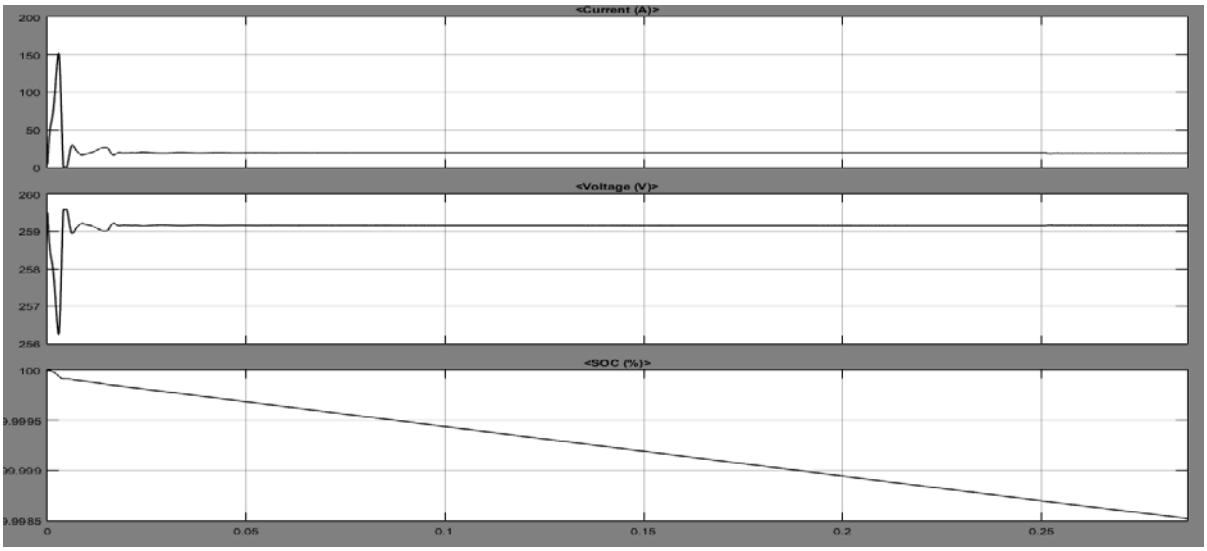

Fig. 14. Current, voltage and SOC of battery

In Fig.14. the case of battery discharge is considered. From the three graphs with time on X-axis and battery current, voltage and SOC on Y-axes respectively, it can be observed that in the duration of 0.3 seconds, the SOC is reducing from 100% which is considered as initial condition to 99.9985%. This depicts that the power is being drawn from the battery.

Having observed the selection criteria and battery charging and discharging, the PQ loop was introduced to control the active and reactive power. Fig. 15 shows the active and reactive power of the three phase 100W load.

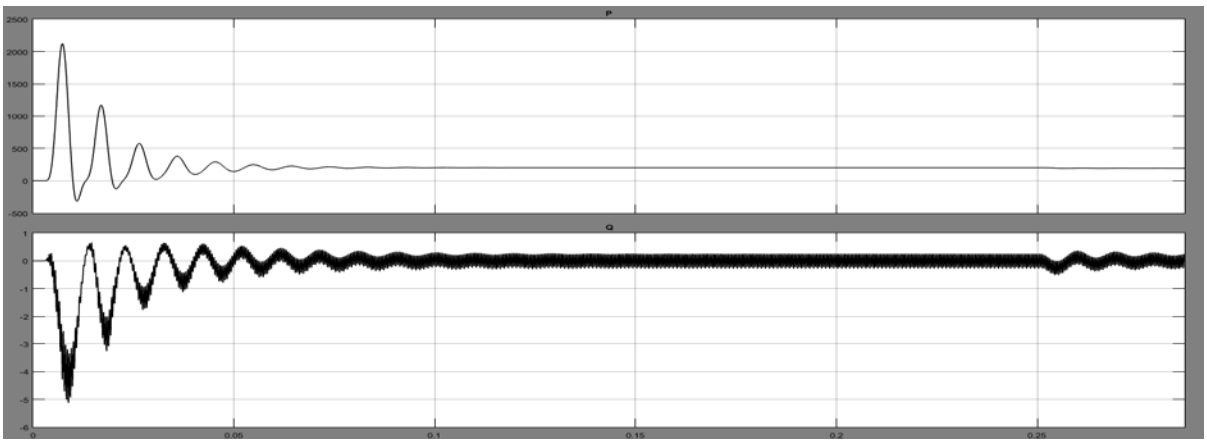

Fig. 15. PQ output without the PQ control loop

Fig. 15 shows without the PQ control loop, the Active and Reactive power on Y-axis and time in seconds on the X-axis. A small change in load of 2W was introduced at 0.25 seconds. The graph shows the impact on the P and Q.

Fig. 16 shows the output active and reactive power with the PQ control loop using 3 PI controllers as suggested in the PQ control strategy. The Active and Reactive power on Y-axis and time in seconds on the X-axis. A small change in load of 2W was introduced at 0.25 seconds. The graph shows no major impact on the P and Q. This demonstrates the control loop being successful in responding to the change in load almost instantaneously.

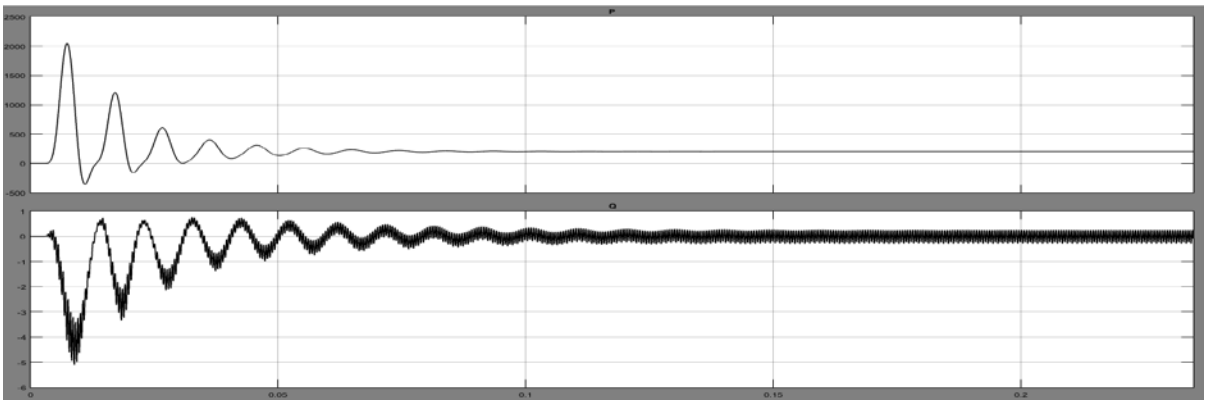

Fig. 16. PQ output with the PQ control loop

For further investigating the results of the implemented PPQ control loop, 2 cases were considered. One when the power generated is greater than the demand. The second when the power generated is less than load.

Case1.

The power generated is greater than its demand, the excess power goes to battery and it charge during islanded operation. The initial SoC of the battery is set at 60%.
Fig. 17 shows the Active and reactive power from time 0 to 1sec.

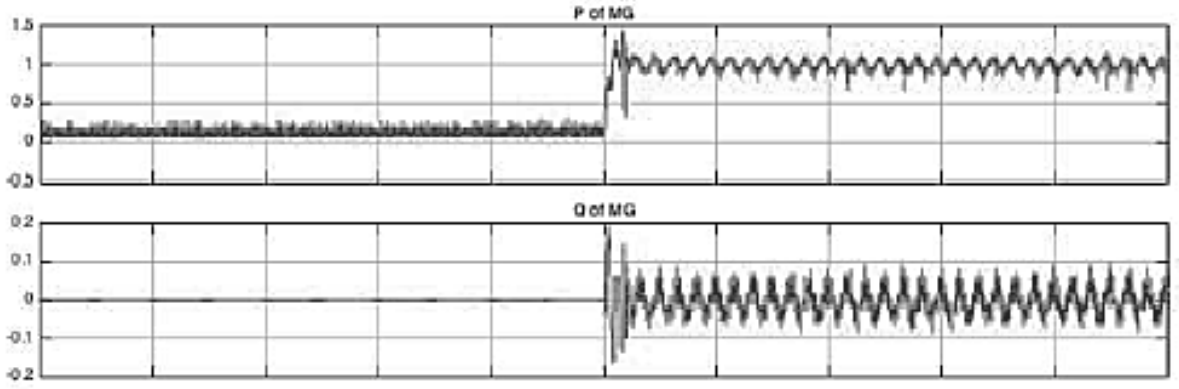

Fig. 17. P and Q of microgrid

On the X-axis time in seconds and on Y-axis pu values of P and Q are displayed. At an instant of 0.5 seconds which is half of simulation time, the load is increased from 1kW to 2kW.

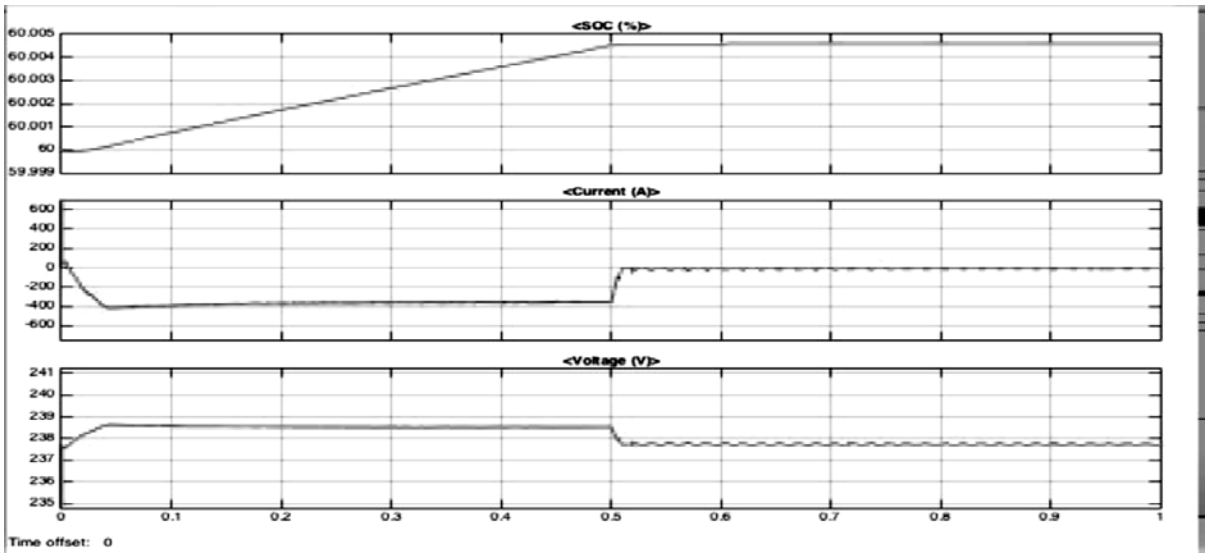

Fig. 18. The battery SOC, current and voltage for case1

Fig. 18 shows that when the load is less and excess power is being generated, charging takes place. When the load becomes almost equal to the supply, the SOC remains the same. Similar observations can be made with current and voltage.

Case 2.

The microgrid load is more than its generated power (300kW) and the deficient power (of 50kW) is supplied by battery as shown in Fig. 19 It can be observed that in this case the battery converter is in boost mode to match the DC link voltage and SOC is decreasing. The P and Q in pu are on Y-axis and time in seconds is on X-axis.

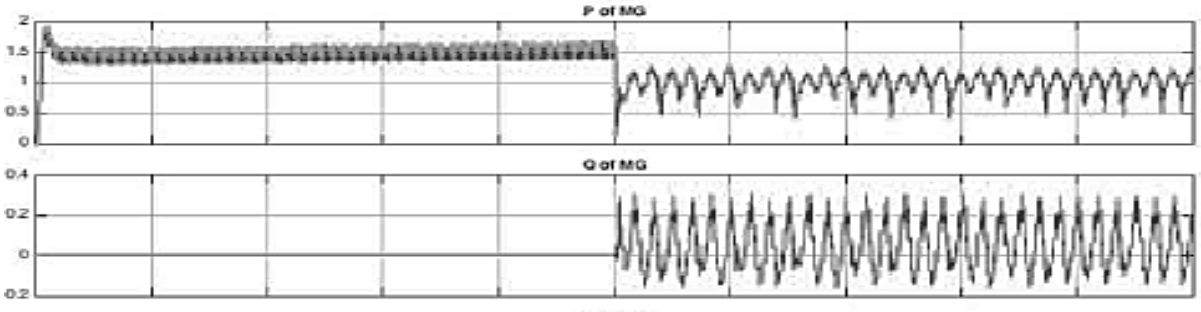

Fig. 19. P and Q of microgrid when load is greater than generated

We can observe that when the load is changed from value greater than generation, the active power difference increases and needs to be supplied by the battery. We can also observe that the reactive power takes longer time to settle. Fig. 20 shows the battery output and SOC

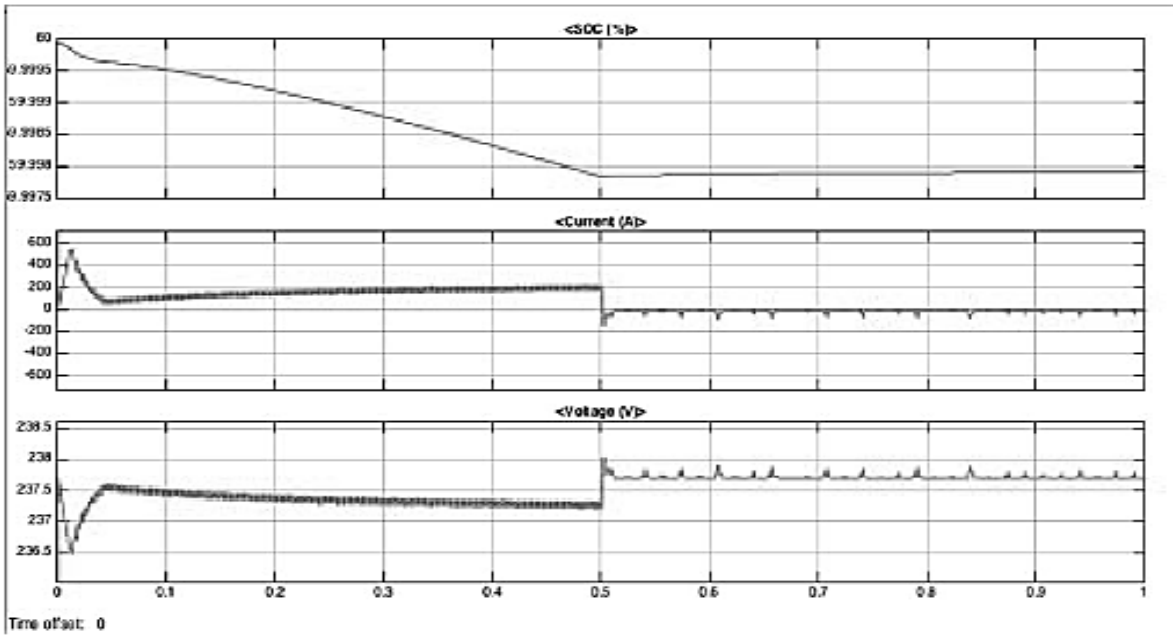

Fig. 20. Battery output and SOC when it is supplying to load

The SOC, current and voltage of battery are on Y-axis and time is on X-axis in Fig. 20. Since the battery is supplying to the load in this case, the SOC is decreasing. The value of voltage and current respectively raise and drop to meet the load demand.

The results when only wind energy conversion system is supplying to the load are demonstrated here. The WECS output is rectified to get a DC output which is connected to the load at the PCC with help of the same inverted used for PV. The output voltage of rectifier is as shown in Fig. 21.

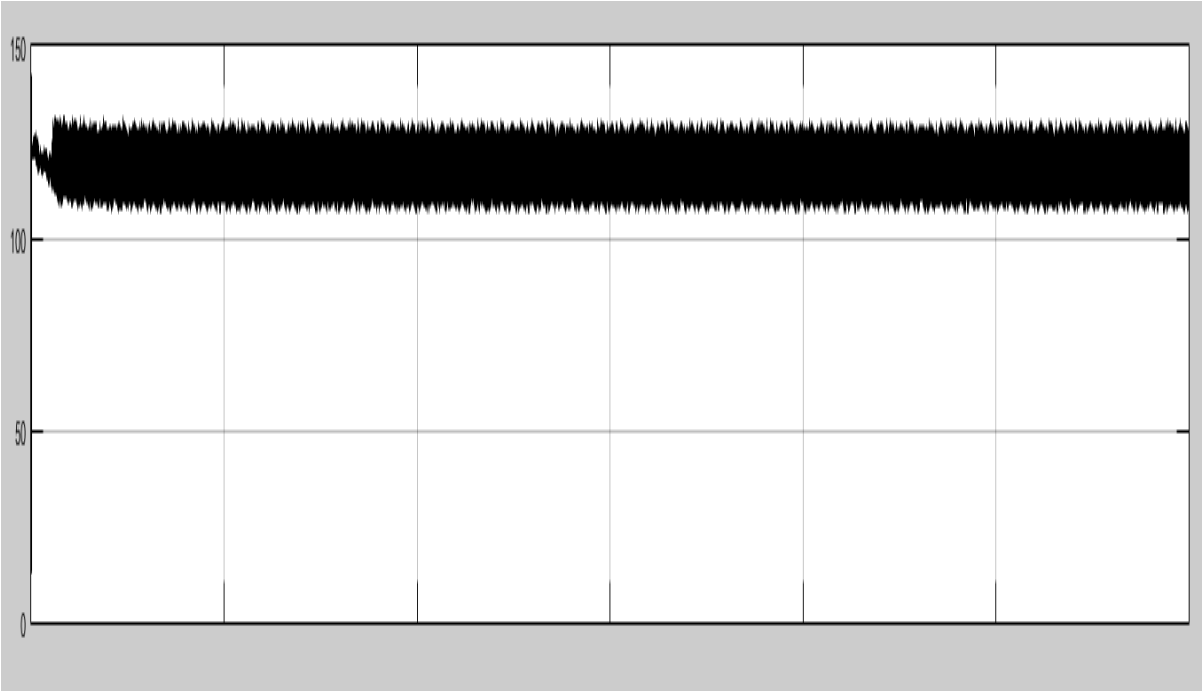

Fig. 21. Output after rectifying the WECS voltage in volts

The axes for Fig. 21 are as follows. The x-axis is the time starting from 0 to 4 seconds which is duration of simulation. The y-axis is the DC voltage in volts. The nominal voltage chosen for the WECS- PMSG is such that it is constant at 120V . The wind speed fed to wind turbine is 12m/s.

In Fig. 22 and Fig. 23 we can observe the active and reactive power in watt and VA respectively being supplied to the RL load. In this figure, the x-axis comprises of the time axis in seconds and y-axis depicts the power in watts. The simulation is carried out for 4 seconds starting from 0. The switch from solar to wind happens at 0.5 seconds which can be observed in the figure.

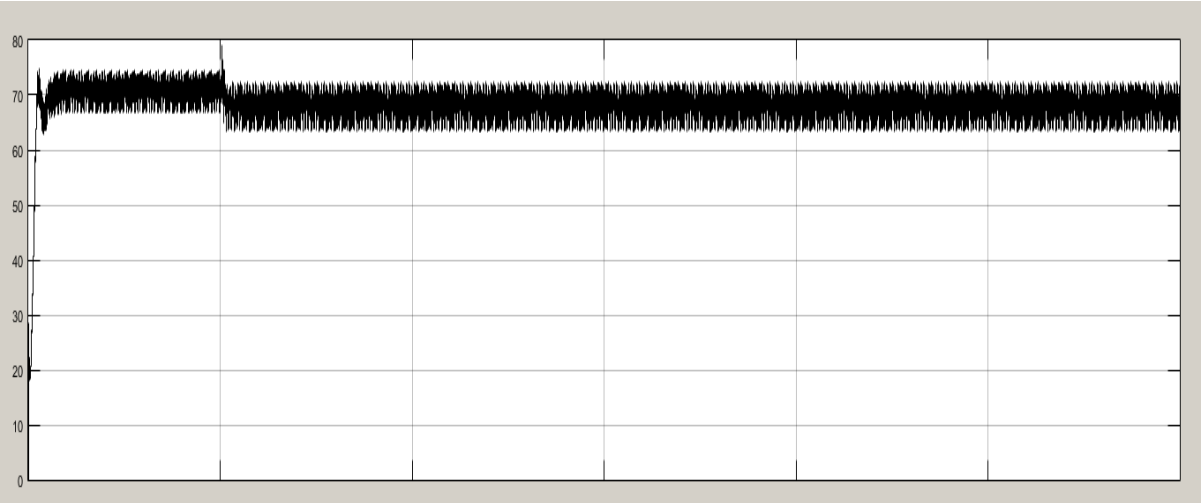

Fig. 22. Active power measured on the load side in watts

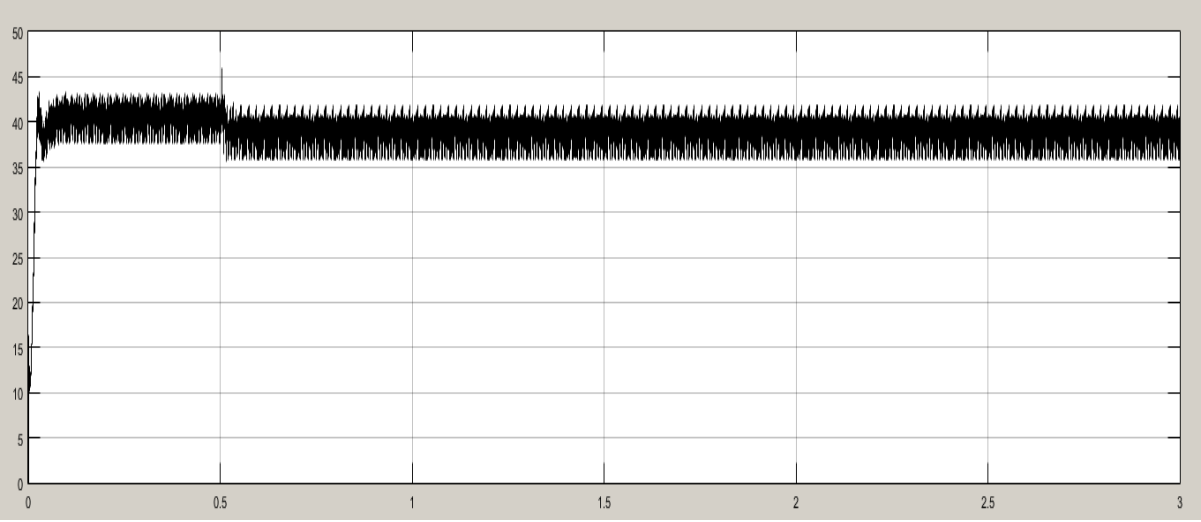

Fig. 23. Reactive power measured on the load side in VA

The real power as measured at the load side when only the WECS is supplying to the load is showed in Fig.24. Real power is computed by taking the rms values of the AC current and voltage on load side.

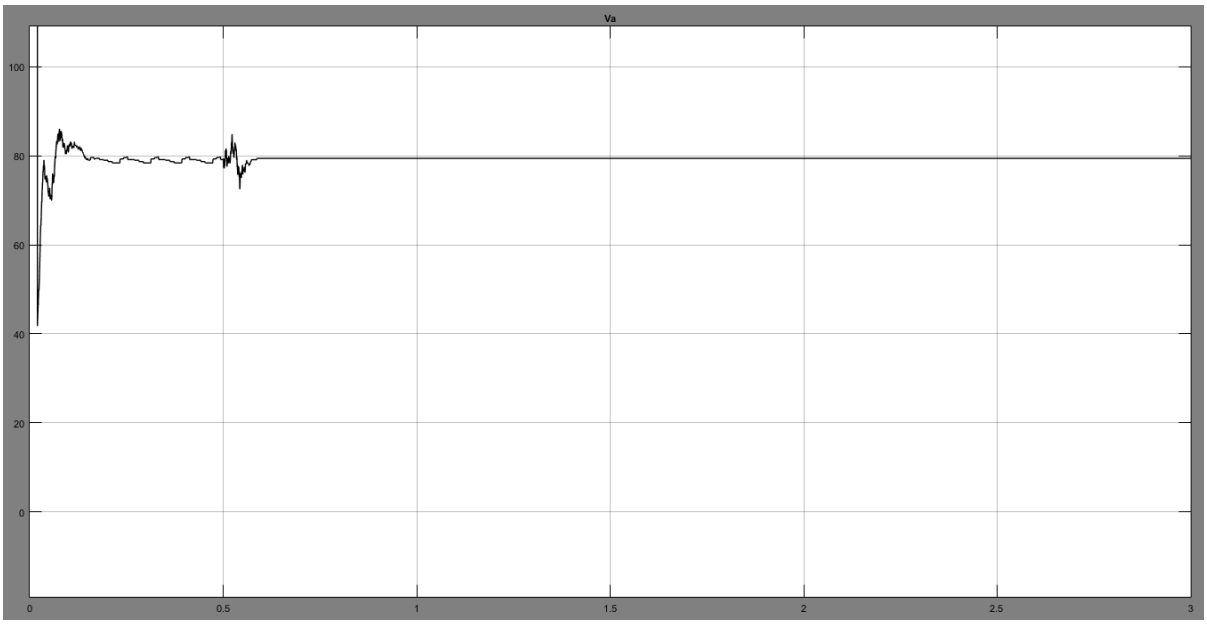

Fig. 24. Real power measured on the load side in watts

The x-axis of Fig.24 shows the time in seconds and y-axis shows power in watts. The sudden change in source supplying to the load can be observed at 0.5 seconds in the figure.

CONCLUSION

A solar with battery backup, WECS and diesel generator powered standalone microgrid which makes use of a Kyocera GT 200 solar panel and a WECS with PMSG was implemented. The system has reliable uninterrupted power supply. The performance of the microgrid was studied under different conditions of weather and load. However the supply voltage to the load is chosen to be 100V which is exclusively to demonstrate the working of this system. With future work, the standard voltage of 480V can be achieved with minor design changes.

References

[1] K. S. Rajesh, S. S. Dash, Bayinder, R. Sridhar, Ragam Rajagopal, "Implementation of an adaptive control strategy for solar photo voltaic generators in microgrlds with MPPT and energy storage" in *IEEE International Conference on Renewable Energy Research and Applications,* 2016, pp. 766- 771.

[2] Sarina Adhikari, Fangxing Li, "Coordinated V-f and P-Q control of solar photovoltaic generators with MPPT and battery storage in microgrids", *IEEE transactions on smart grid,* 2014, vol.5 no. 3

[3] R. H. Lasseter, "MicroGrids," in *Proc. IEEE Power Engineering Society Winter Meeting*, 2002, vol. 1, pp. 305–308.

[4] S. Chowdhury, S. P. Chowdhury, and P. Crossley, "Microgrids and ActiveDistribution Networks," 2009, IET Renewable Energy Series 6.

[5] H. Saadat, *Power System Analysis*, 2nd ed. New York, NY, USA:Mc- Graw Hill, 2002.

[6] J. A. P. Lopes, C. L. Moreira, and A. G. Madureira, "Defining control strategies for MicroGrids islanded operation," *IEEE Trans. Power Syst.*, vol. 21, pp. 916–924, 2006.

[7] B. Awad, J.Wu, and N. Jenkins, "Control of distributed generation," *Electrotechn. Info. (2008)*, vol. 125/12, pp. 409–414.

[8] J. C. Vasquez, J. M. Guerrero, E. Gregorio, P. Rodriguez, R. Teodorescu, and F. Blaabjerg, "Adaptive droop control applied to distributed generation inverters connected to the grid," in *Proc. 2008 IEEE ISIE*, pp. 2420–2425.

[9] H. Bevrani and S. Shokoohi, "An intelligent droop control for simultaneous voltage and frequency regulation in islanded microgrids," *IEEE Trans. Smart Grid*, vol. 4, no. 3, pp. 1505–1513, Sep. 2013.

[10] J. C. Vasquez, J. M. Guerrero, M. Savaghebi, and R. Teodorescu, "Modelling, analysis and design of stationary reference frame droop controlled parallel three-phase voltage source inverters," in *Proc. 2011 IEEE 8th ICPE & ECCE*, pp. 272–279.

[11] T. L. Vandoorn, B. Meersman, J. D. M. De Kooning, and L. Vandevelde, "Analogy between conventional grid contro and islanded microgrid control based on a global DC-link voltage droop," *IEEE Trans. Power Delivery*, vol. 27, no. 3, pp. 1405–1414, Jul. 2012.

[12] H. Laaksonen, P. Saari, and R. Komulainen, "Voltage and frequency control of inverter based weak LV network microgrid," presented at the Int. Conf. Future Power Syst., Amsterdam, The Netherlands, Nov. 18, 2005.
[13] J. C. Vasquez, R. A. Mastromauro, J. M. Guerrero, and M. Liserre, "Voltage support provided by a droop-controlled multifunctional inverter," *IEEE Trans. Ind. Electron.*, vol. 56, pp. 4510–4519, 2009.
[14] H. Li, F. Li, Y. Xu, D. T. Rizy, and J. D. Kueck, "Adaptive voltage control with distributed energy resources: Algorithm, theoretical analysis, simulation and field test verification," *IEEE Trans. Power Syst.*, vol. 25, pp. 1638–1647, Aug. 2010.
[15] H. Li, F. Li, Y. Xu, D. T. Rizy, and S. Adhikari, "Autonomous and adaptive voltage control using multiple distributed energy resources," *IEEE Trans. Power Syst.*, vol. 28, no. 2, pp. 718–730, May 2013.
[16] L. D.Watson and J.W. Kimball, "Frequency regulation of a microgrid using solar power," in *Proc. 2011 IEEE APEC*, pp. 321–326.
[17] M. G. Molina and P. E. Mercado, "Modeling and control of grid-connected photovoltaic energy conversion system used as a dispersed generator," in *Proc. 2008 IEEE/PES Transm. Distrib. Conf. Expo.: Latin America*, pp. 1–8.
[18] N. Kakimoto, S. Takayama, H. Satoh, and K. Nakamura, "Power modulation of photovoltaic generator for frequency control of power system," *IEEE Trans. Energy Conv.*, vol. 24, pp. 943–949, 2009.
[19] T. Ota, K. Mizuno, K. Yukita, H. Nakano, Y. Goto, and K. Ichiyanagi, "Study of load frequency control for a microgrid," in *Proc. 2007AUPEC Power Eng. Conf.*, pp. 1–6.
[20] L. Xu, Z. Miao, and L. Fan, "Coordinated control of a solar battery system in amicrogrid," in *Proc. 2012 IEEE/PES Transm. Distrib. Conf. Expo. (T&D)*, pp. 1–7.
[21] M. G. Villalva, J. R. Gazoli, and E. R. Filho, "Comprehensive approach to modeling and simulation of photovoltaic arrays," *IEEE Trans. Power Electron.*, vol. 24, no. 5, pp. 1198–1208, 2009.
[22] Y. Xu, H. Li, D. T. Rizy, F. Li, and J. D. Kueck, "Instantaneous active and nonactive power control of distributed energy resources with a current limiter," in *Proc. IEEE Energy Conversion Congr. Expo.*, 2010, pp. 3855–3861.
[23] O. Tremblay and L. A. Dessaint, "Experimental validation of a battery dynamic model for EV applications," *World Electric Vehicle J.*, vol. 3, 2009.
[24] Y. Xu, F. Li, D. T. Rizy, and J. D. Kueck, "Active and non active power control with distributed energy resources," in *Proc. 2008 40th North American Power Symp. NAPS'08*, pp. 1–7.
[25] S. Adhikari *et al.*, "Utility-side voltage and PQ control with inverter based photovoltaic systems," in *Proc. 18th World Congr. IFAC*,Milan, Italy, Aug. 28–Sep. 2 2011, pp. 6110–6116.
[26] Smita Sugriv Gite, S. H. Pawar, "Modeling of wind energy system with MPPT control for DC microgrid", 2017, in *Second International Conference on Electrical, Computer and Communication Technologies (ICECCT)*,pp: 1 - 6
[27] Weiqiang Liu, Chaoxu Mu, Ding Wang, Chao Luo, Chao Ren, "Neural adaptive control of microgrid frequency regulation with wind power", in *43rd Annual Conference of the IEEE Industrial Electronics Society*, 2017 pp: 7451 – 7456